

Voltage-sensitive dyes for monitoring multineuronal activity in the intact central nervous system

JIAN-YOUNG WU¹, YING-WAN LAM², CHUN X. FALK^{2,5},
LAWRENCE B. COHEN^{2,5}, JING FANG², LESLIE LOEW³, JAMES C. PRECHTL⁴,
DAVID KLEINFELD⁴ and YANG TSAU¹

¹Georgetown Institute of Cognitive and Computational Sciences, Georgetown University, Washington, DC, 20007; ²Department of Cellular and Molecular Physiology, Yale University School of Medicine, New Haven, CT 06520; ³Department of Physiology, University of Connecticut Health Center, Farmington, CT 06032; and ⁴Department of Physics 0319, University of California, La Jolla, CA 92093; ⁵OptImaging, LLC, Fairfield, CT 06432, USA

Received 28 October 1997

Summary

Optical monitoring of activity provides new kinds of information about brain function. Two examples are discussed in this article. First, the spike activity of many individual neurons in small ganglia can be determined. Second, the spatio-temporal characteristics of coherent activity in the brain can be directly measured. This article discusses both general characteristics of optical measurements (sources of noise) as well as more methodological aspects related to voltage-sensitive dye measurements from the nervous system.

© 1998 Chapman & Hall

Introduction

An optical measurement of membrane potential using a molecular probe can be beneficial in a variety of circumstances. In particular, this kind of measurement offers the possibility of simultaneous measurements from many locations. This is especially important in the study of nervous systems in which many parts of cells or cells or regions are simultaneously active. In addition, optical recording offers the possibility of recording from processes that are too small or fragile for electrode recording.

All of the optical signals described in this paper are 'fast' signals (Cohen & Salzberg, 1978). These signals are presumed to arise from membrane-bound dye; they follow changes in membrane potential with time courses that are rapid compared with the rise time of an action potential. Several voltage-sensitive dyes (see Fig. 1) have been used to monitor changes in potential in a variety of preparations. Two topics have been discussed in detail in earlier reviews and will not be covered here: (1) evidence showing that these optical signals are potential dependent; and (2) evidence that pharmacological effects and photodynamic damage resulting from the voltage-sensitive dyes are manageable (see Cohen & Salzberg, 1978; Waggoner, 1979; Salzberg, 1983; Grinvald *et al.*, 1988). Earlier descrip-

tions of methods have been published (Cohen & Leshner, 1986; Grinvald *et al.*, 1988; Wu & Cohen, 1993).

We begin with a discussion of signal type, dyes, light sources, photodetectors, optics and computer hardware and software. This concern about apparatus arises because the signal-to-noise ratios in optical measurements are often small, and attention to detail is required to achieve optimal results. While some of the discussion is most relevant to our own apparatus, other aspects would apply to any optical measurement.

The second half of the article will describe the experimental details and examples of results obtained from two kinds of voltage-sensitive dye measurements. First, measurements of the action potential signals of individual neurons and, secondly, population signals representing the average change in membrane potential from many cells and processes. In both instances, optical recordings have provided kinds of information about the function of the nervous system that were previously unobtainable.

Signal type

Sometimes, it is possible to decide in advance which kind of optical signal will give the best signal-to-noise

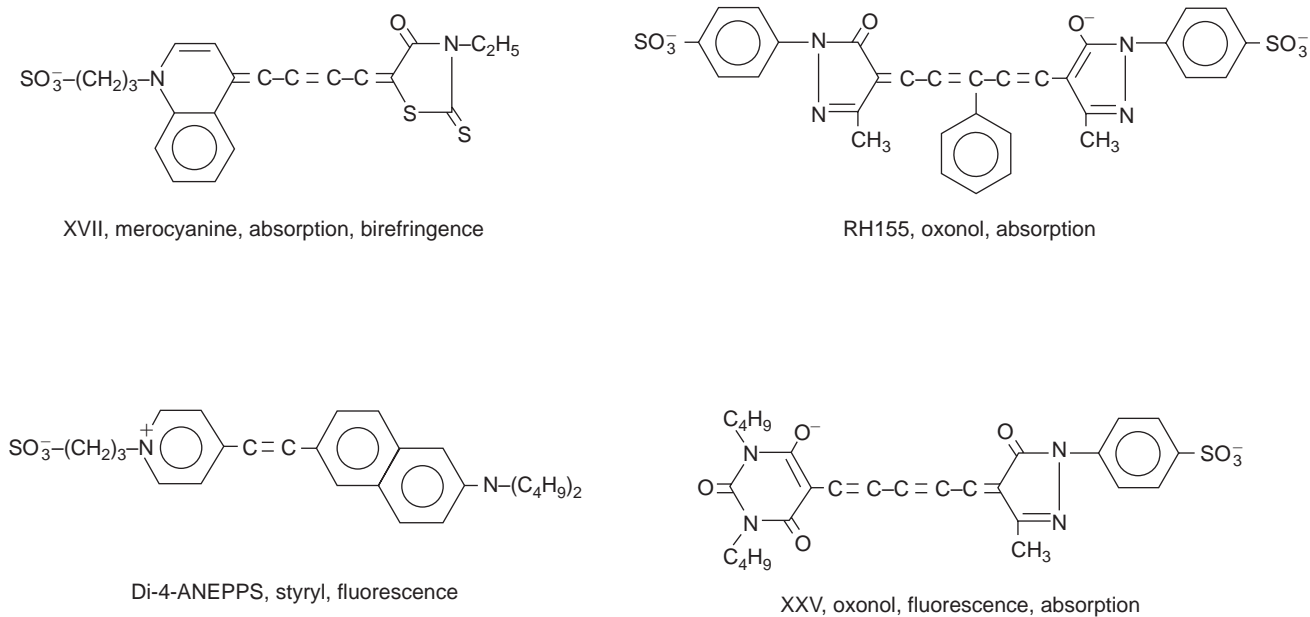


Fig. 1. Examples of four different chromophores that have been used to monitor membrane potential. The merocyanine dye, XVII (WW375), and the oxonol dye, RH155, are commercially available as NK2495 and NK3041 from Nippon Kankoh-Shikiso Kenkyusho Co., Okayama, Japan. The oxonol, XXV (WW781), and styryl, di-4-ANEPPS, are available commercially as dye R-1114 and D-1199 from Molecular Probes, Junction City, OR, USA.

ratio but, in other situations, an experimental comparison is necessary. The choice of signal type often depends on the optical characteristics of the preparation. Birefringence signals are relatively large in preparations that, like giant axons, have a cylindrical shape and radial optical axis. However, in preparations with spherical symmetry (e.g. molluscan cell soma), the birefringence signals in adjacent quadrants will cancel (Boyle & Cohen, 1980). In one experiment to which birefringence should have been tested, it was not (Shrager *et al.*, 1987).

Thick preparations (e.g. mammalian cortex) also dictate the choice of signal. In these circumstances transmitted light measurements are not easy (a subcortical implantation of a light guide would be necessary), and the small size of the absorption signals that are detected in reflected light (Ross *et al.*, 1974; Orbach & Cohen, 1983) mean that fluorescence will be optimal (Orbach *et al.*, 1985). Blasdel and Salama (1986) claimed the dye-related reflectance changes can be measured from cortex; however, Grinvald *et al.* (1986) suggests that these slow signals are caused by a change in intrinsic reflectance.

Another factor that affects the choice of absorption or fluorescence is that the signal-to-noise ratio in fluorescence is more strongly degraded by dye bound to extraneous material. Fig. 2 illustrates a spherical cell surrounded by extraneous material. In Fig. 2A, dye binds only to the cell; in Fig. 2B, there is 10 times as much dye bound to extraneous material. To calculate the transmitted intensity, we assume

that there is one dye molecule for every 2.5 phospholipid molecules and a large extinction coefficient (10^5). The amount of light absorbed by the cell is still only 0.01 of the incident light and, thus the transmitted light is 0.99 I_0 . Thus, even if this dye completely disappeared as a result of a change in potential, the fractional change in transmission, $\Delta I/I_0$, would be only 1% (10^{-2}). The amount of light reaching the photodetector in fluorescence will be much lower, say 0.0001 I_0 . But, even though the light reaching the fluorescence detector is small, disappearance of dye would result in a 100% decrease in fluorescence, a fractional change of 100. Thus, in situations in which dye is bound only to the cell membrane and there is only one cell in the light path, the fractional change in fluorescence is much larger than the fractional change in transmission.

However, the relative advantage of fluorescence is reduced if dye binds to extraneous material. When 10 times as much dye is bound to the extraneous material as is bound to the cell membrane (Fig. 2B), the transmitted intensity is reduced to approximately 0.9 I_0 , but the fractional change in transmission is nearly unaffected. In contrast, the resting fluorescence is now higher by a factor of 10, and the fractional fluorescence change is reduced by the same factor. It does not matter whether the extraneous material happens to be connective tissue, glial membrane or neighbouring neuronal membranes.

In Fig. 2B, the fractional change in fluorescence was still larger than in transmission. However, in

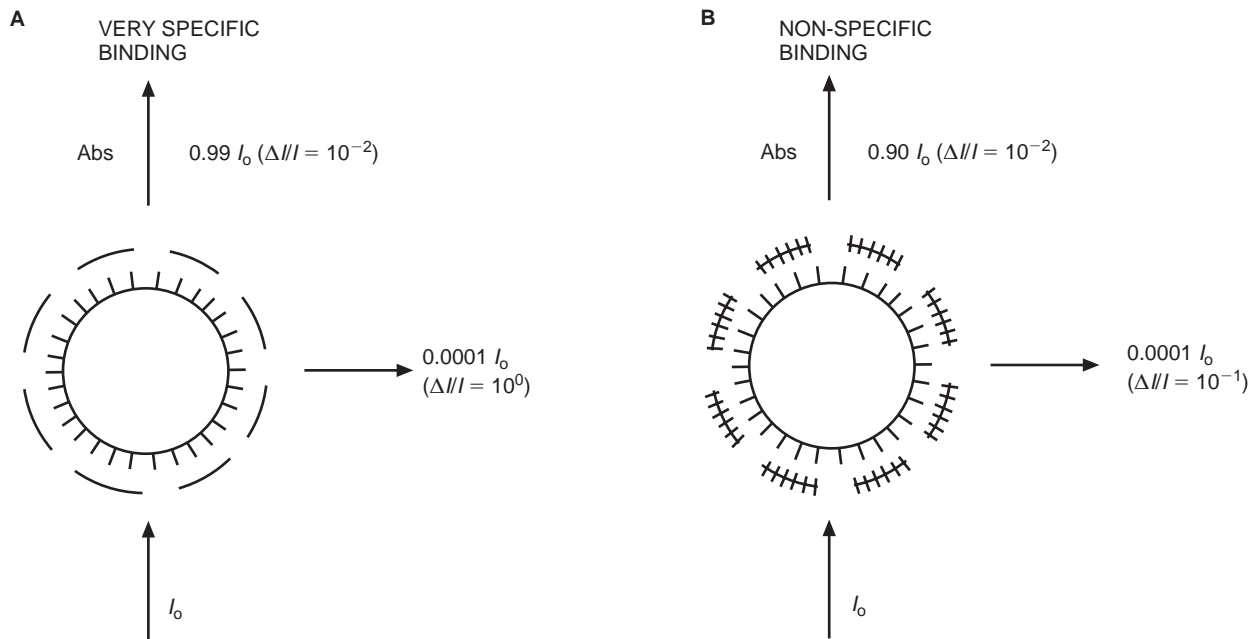


Fig. 2. (A) The light transmission and fluorescence intensity when only a neuron binds dye and (B) when both the neuron and extraneous material binds dye. In (A), assuming that one dye molecule is bound per 2.5 phospholipid molecules, 0.99 of the incident light is transmitted. If a change in membrane potential causes the dye to disappear, the fractional change in transmission is 1%, but in fluorescence it is 100%. In (B), nine times as much dye is bound to extraneous material. Now the transmitted intensity is reduced to 0.9, but the fractional change is still 1%. The fluorescence intensity is increased 10-fold and, therefore, the fractional change is reduced by the same factor. Thus, extraneously bound dye degrades fluorescence fractional changes and signal-to-noise ratios more rapidly. Redrawn from Cohen & Leshner (1986).

fluorescence, the light intensity was about 10^3 smaller, which reduces the signal-to-noise ratio. Partly because of the signal degradation resulting from extraneous dye, fluorescence signals have been used most often in monitoring activity from tissue-cultured neurons, whereas absorption has been preferred in measurements from ganglia. Both kinds of signals have been used in brain slices. The discovery of methods for neuron type-specific staining (see below) makes the use of fluorescence more attractive.

Dyes

The choice of dye is important in maximizing the signal-to-noise ratio. Using giant axons, more than 1500 dyes have been tested for signal size in absorption and fluorescence. This screening was made possible by the synthetic efforts of three laboratories: Jeff Wang, Ravender Gupta and Alan Waggoner then at Amherst College; Rina Hildesheim and Amiram Grinvald at the Weizmann Institute; and Joe Wuskell and Leslie Loew at the University of Connecticut Health Center. Included in these syntheses were about 100 analogues of each of the four dyes illustrated in Fig. 1. In each of these four groups, there were 10 or 20 dyes that gave

approximately the same signal size on squid axons (Gupta *et al.*, 1981).

However, dyes that gave nearly identical signals on squid axons gave very different responses on other preparations and, thus, tens of dyes had to be tested to maximize the signal. Examples of preparations in which a number of dyes had to be screened are the *Navanax* and *Aplysia* ganglia (London *et al.*, 1987; Zecevic *et al.*, 1989; Morton *et al.*, 1991), mammalian cortex (Orbach *et al.*, 1985; Grinvald *et al.*, 1994), tissue-cultured neurons (Ross & Reichardt, 1979; Grinvald *et al.*, 1981) and embryonic chick spinal cord (Tsau *et al.*, 1996). Some dyes that worked well in squid did poorly in other preparations, because they do not penetrate through connective tissue or along intercellular spaces to the membrane of interest. Others dyes appeared to have a relatively low affinity for neuronal versus non-neuronal tissue. Finally, in some cases, the dye penetrated well and the staining appeared to be specific, but nonetheless the signals were small.

Better dyes?

The dyes in Fig. 1 and the vast majority of those synthesized in recent years are of the general class named polyenes (Hamer, 1964), a group that is used to extend the wavelength response of photographic

film. It is possible that improvements in signal size can be obtained with new polyene dyes (see Waggoner & Grinvald, 1977 and Fromherz *et al.*, 1991 for a discussion of maximum possible fractional change in absorption and fluorescence). On the other hand, the fractional change on squid axons has not increased in recent years (Gupta *et al.*, 1981; L. B. Cohen, A. Grinvald, K. Kamino and B. M. Salzberg, unpublished results), and most improvements (e.g. Grinvald *et al.*, 1982a; Momose-Sato *et al.*, 1995; Antic & Zecevic, 1995; Tsau *et al.*, 1996) have involved synthesizing analogues that work well on new preparations. Radically different kinds of molecules might prove to be useful (see below).

Amplitude of the voltage change

All of the voltage-sensitive dye signals discussed in this article are simple changes in intensity (ΔI) or the fractional intensity change ($\Delta I/I$). These signals give information about the time course of the potential change but no direct information about its magnitude. In some instances, indirect information about the magnitude of the voltage change underlying the optical signal can be obtained (e.g. Orbach *et al.*, 1985; Delaney *et al.*, 1994; Antic & Zecevic, 1995). Another approach is the use of ratiometric measurements at two independent wavelengths (Gross *et al.*, 1994). However, to determine the amplitude of the voltage change from a ratio measurement, one must know the fraction of the fluorescence that results from dye not bound to active membrane, a requirement that can only be met in special circumstances (e.g. tissue culture).

Attempts to use optical properties other than birefringence, absorption and fluorescence are discussed below.

Measuring technology

Noise

Shot noise. The limit of accuracy with which light can be measured is set by the shot noise arising from the statistical nature of photon emission and detection. Fluctuations in the number of photons emitted per unit time will occur and if an ideal light source (tungsten filament at 3300 °F) emits an average of 10^{14} photons ms^{-1} , the root-mean-square (RMS) deviation in the number emitted is the square root of this number or 10^7 photons ms^{-1} . In the shot noise-limited case, the signal-to-noise ratio is proportional to the square root of the number of measured photons and the bandwidth of the photodetection system (Braddick, 1960; Malmstadt *et al.*, 1974). The basis for the square root dependence on intensity is illustrated in Fig. 3. In Fig. 3A, the result of using a random number table to distribute 20 photons into 20 time windows

is shown. In Fig. 3B, the same procedure was used to distribute 200 photons into the same 20 bins. Relative to the average light level, there is more noise in the top trace (20 photons) than in the bottom trace (200 photons). On the right side of Fig. 3, the signal-to-noise ratios are measured, and the improvement is similar to that expected from the square root relationship. This relationship is indicated by the dotted line in Fig. 4. In a shot noise-limited measurement, improvements in the signal-to-noise ratio can only be obtained by: (1) increasing the illumination intensity; (2) improving the light-gathering efficiency of the measuring system; or (3) reducing the system bandwidth.

Because only a small fraction of the 10^{14} photons ms^{-1} emitted by a tungsten filament will be measured, a signal-to-noise ratio of 10^7 (see above) cannot be achieved. A partial listing of the light losses follows. A 0.7-NA lamp collector lens would collect 0.06 of the light emitted by the source. Only 0.2 of that light is in the visible wavelength range; the remainder is infrared (heat). An interference filter of 30-nm width at half-height might transmit only 0.05 of the visible light. Finally, additional losses will occur at all air-glass interfaces. Thus, the light reaching the preparation might typically be reduced to 10^{10} photons ms^{-1} . If the light-collecting system has high efficiency, e.g. in an absorption measurement, about 10^{10} photons ms^{-1} will reach the photodetector and, if the photodetector has a quantum efficiency of 1.0, then 10^{10} photoelectrons ms^{-1} will be measured. The RMS shot noise will be 10^5 photoelectrons ms^{-1} ; thus, the relative noise is 10^{-5} (a signal-to-noise ratio of 100 db).

Extraneous noise. A second type of noise, termed extraneous or technical noise, is more apparent at higher light intensities where the sensitivity of the measurement is high because the fractional shot noise and dark noise are low. One type of extraneous noise is caused by fluctuations in the output of the light source (see below). Two other sources of extraneous noise are vibrations and movement of the preparation. A number of precautions for reducing vibrational noise are described in Salzberg *et al.* (1977). In addition, embedding ganglia in 1–3% agar reduced vibrational noise (London *et al.*, 1987). The pneumatic isolation mounts on vibration isolation tables are more efficient in reducing vertical vibrations than in reducing horizontal movements. We now use air-filled soft rubber tubes (Newport Corporation, Irvine, CA, USA) or a combination of pneumatic isolation mounts and tubes. Nevertheless, it has been difficult to reduce vibrational noise to less than 10^{-5} of the total light. With this amount of vibrational noise, increases in measured intensity beyond

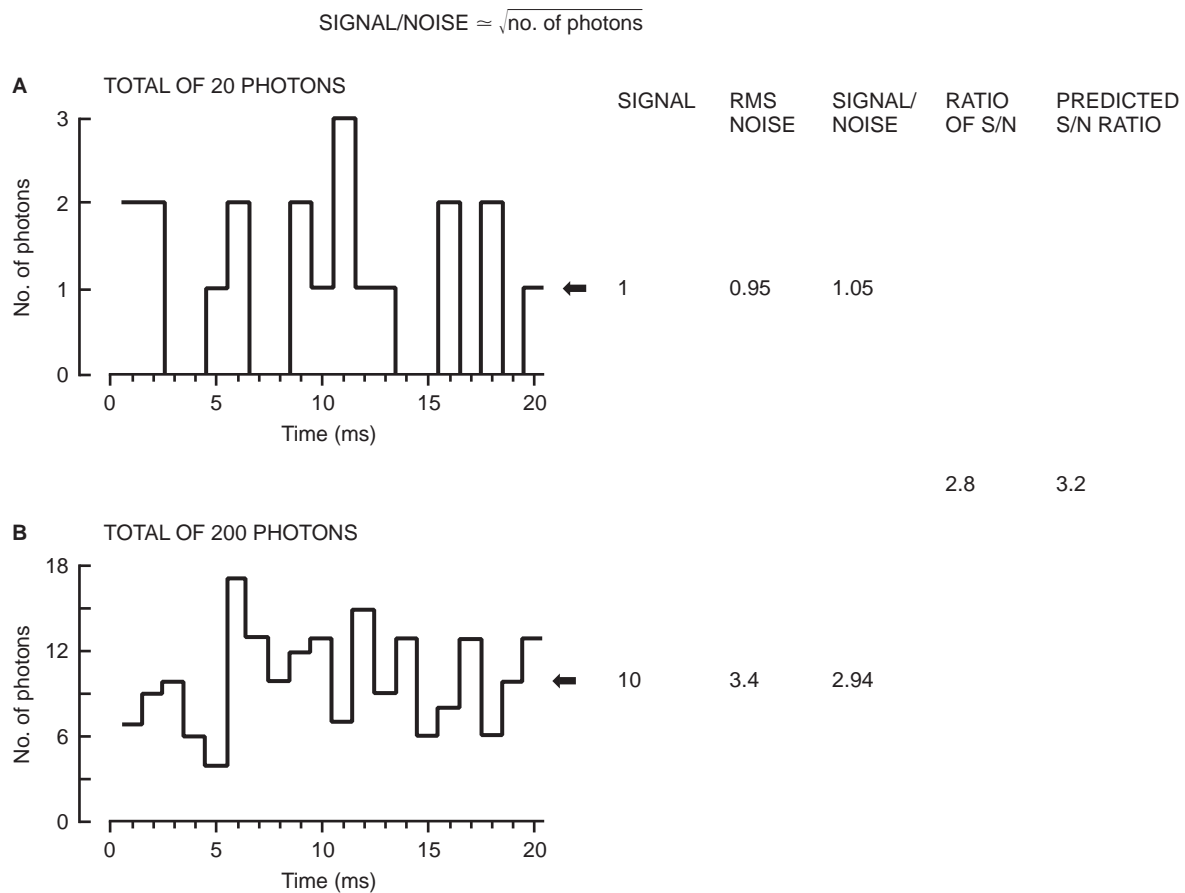


Fig. 3 Plots of the results of using a table of random numbers to distribute 20 photons (top, A) or 200 photons (bottom, B) into 20 time bins. The result illustrates the fact that, when more photons are measured, the signal-to-noise ratio is improved. On the right, the signal-to-noise ratio is measured for the two results. The ratio of the two signal-to-noise ratios was 2.8. This is close to the ratio predicted by the relationship that the signal-to-noise ratio is proportional to the square root of the measured intensity. Redrawn from Wu & Cohen (1993).

10^{10} photons ms^{-1} would not improve the signal-to-noise ratio (segment C of Fig. 4).

Noise caused by movement of the preparation is a potential problem in *in vivo* measurements. The use of agar to reduce the movements in molluscan preparations is described in London *et al.* (1987). Methods used in mammalian preparations are described below.

Dark noise. Dark noise will degrade the signal-to-noise ratio at low light levels (segment A of Fig. 4).

Light sources

Three kinds of sources have been used. Tungsten filament lamps are a stable source, but their intensity is relatively low, particularly at wavelengths less than 480 nm. Arc lamps are somewhat less stable but can provide more intense illumination. Until recently, measurements made with laser illumination have been substantially noisier.

Tungsten filament lamps. It is not difficult to provide a power supply stable enough so that the output of

the bulb fluctuates by less than 1 part in 10^5 . In absorption measurements, where the fractional changes in intensity are relatively small, only tungsten filament sources have been used. On the other hand, fluorescence measurements often have larger fractional changes that will tolerate light sources with systematic noise better, and the measured intensities are low, making improvements in signal-to-noise ratio from brighter sources attractive.

Arc lamps. Opti-Quip provides 150- and 250-W xenon power supplies, lamp housing and arc lamps with noise that is in the range 1 part in 10^{-4} (item 1 in Approximate costs). In our apparatus, the 150-W bulb yielded 2–3 times more light at 520 ± 45 nm than a tungsten filament bulb and, in turn, the 250-W bulb was 2–3 times brighter than the 150-W bulb. The extra intensity is especially useful for fluorescence measurements from single neurons. If the dark noise is dominant, then the signal-to-noise ratio will improve linearly with intensity and, if the shot noise is dominant, it will improve as the square root of intensity (Fig. 4).

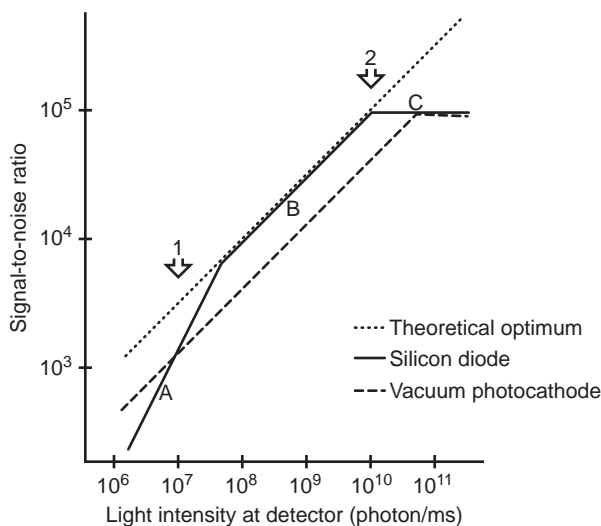


Fig. 4 Signal-to-noise ratio as a function of light intensity in photons ms^{-1} . The approximate light intensity per detector in fluorescence measurements from an individual neuron is indicated by arrow 1. The approximate intensity in absorption measurements in ganglia or brain slices is indicated by arrow 2. The theoretical optimum signal-to-noise ratio (dotted line) is the shot noise limit. The signal-to-noise ratio expected with a silicon diode detector is indicated by the solid line. The silicon diode signal-to-noise ratio approaches the theoretical maximum at intermediate light intensities (segment B) but falls off at low intensities (segment A) because of dark noise, and falls off at high intensities (segment C) because of extraneous noise. The expected signal-to-noise ratio for a vacuum photocathode detector is indicated by the dashed line. At low intensities the vacuum photocathode is better than a silicon diode, because it has less dark noise. At intermediate intensities it is not as good because of its lower quantum efficiency. Redrawn from Cohen & Leshner (1986).

Lasers. It has been possible to take advantage of two useful characteristics of laser sources. First, in preparations with minimal light scattering, the laser output can be focused onto a small spot allowing measurement of membrane potential from small processes in tissue-cultured neurons (Grinvald & Farber, 1981). Secondly, the laser beam can be positioned flexibly and rapidly using acousto-optical deflectors (see below). However, there may be excess noise, which may be caused by laser speckle (Dainty, 1984).

Optics

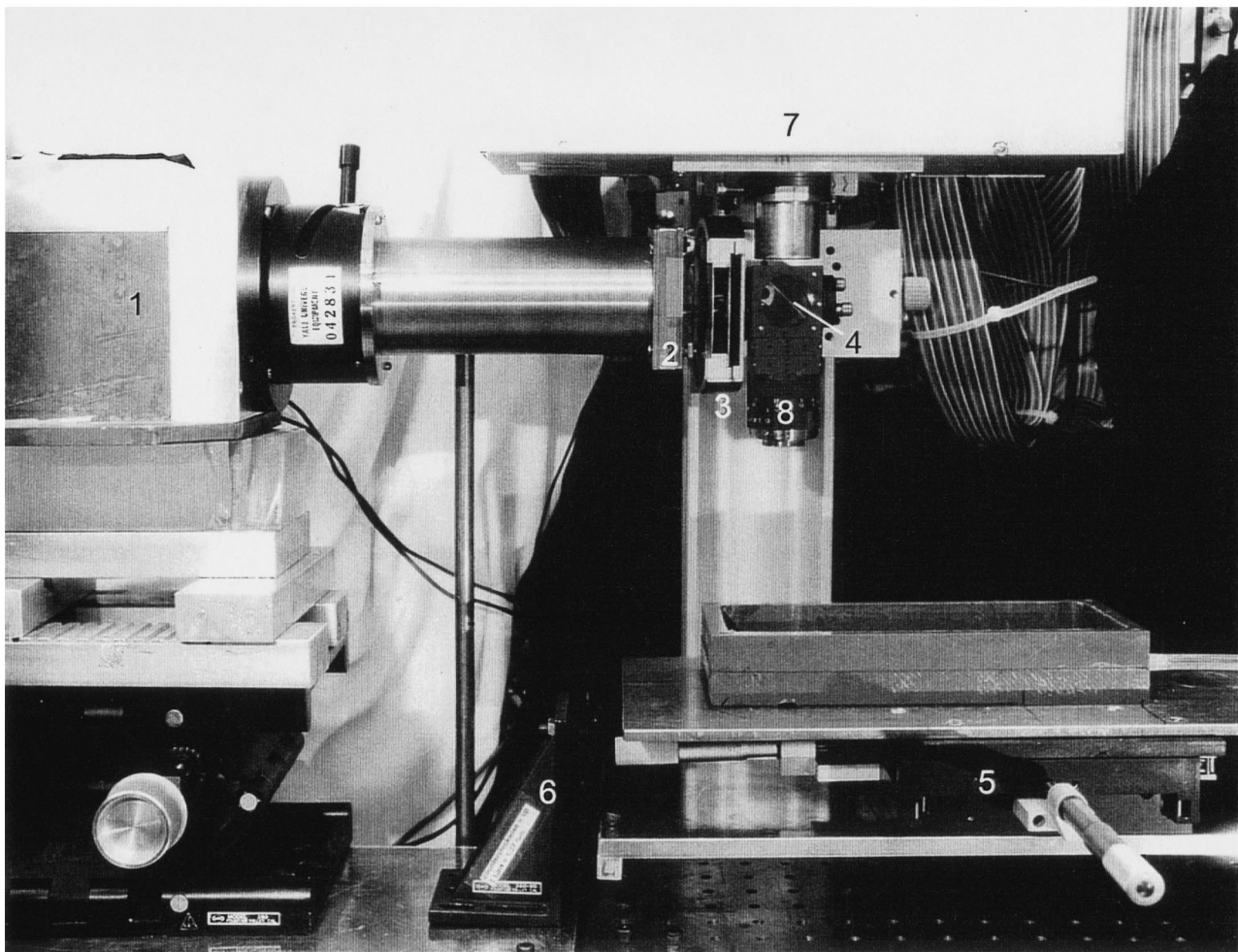
Numerical aperture. The need to maximize the number of measured photons has also been a dominant factor in the choice of optical components. The number of photons collected by an objective lens in forming the image is proportional to the square of the numerical aperture (NA). In epifluorescence,

both the excitation light and the emitted light pass through the objective, and the intensity reaching the photodetector is proportional to the fourth power of NA. Accordingly, objectives (and condensers) with high numerical apertures have been employed. Unfortunately, conventional microscope optics have low numerical apertures at low magnifications. Salama (1988), Ratzlaff and Grinvald (1991), and Kleinfeld and Delaney (1996) took advantage of the high NA that can be achieved by using a camera lens in place of a microscope objective. Fig. 5 illustrates a microscope that we assembled based on a 25-mm focal length, 0.95 f, C-mount, camera lens (item 2 in Approximate costs). With a (item 2 in Approximate costs) magnification of 4 \times , the intensity reaching the photodetector was 100 times larger with this microscope than with our conventional microscope.

Objective efficiency. Direct comparison of the intensity reaching the image plane has shown that the light-collecting efficiency of an objective is not completely determined by the stated magnification and NA. We recommend empirical tests of several lenses for efficiency.

Depth of focus. Salzberg *et al.* (1977) determined the effective depth of focus for a 0.4-NA objective lens by recording an optical signal from a neuron when it was in focus and then moving the neuron out of focus by various distances. They found that the neuron had to be moved 300 μm out of focus to cause a 50% reduction in signal size. (This result will be obtained only when the diameter of the neuron image and the diameter of the detector are similar.) Using 0.5-NA optics, 100 μm out of focus led to a reduction of 50% (Kleinfeld & Delaney, 1996).

Light scattering and out-of-focus light. Light scattering can limit the spatial resolution of an optical measurement. London *et al.* (1987) measured the scattering of 705-nm light in *Navanax* buccal ganglia. They found that inserting a ganglion in the light path caused light from a 30- μm spot to spread so that the diameter of the circle of light that included intensities greater than 50% of the total was roughly 50 μm . The spread was greater, to about 100 μm , with light of 510 nm. As the blurring is not large compared with the average cell diameter at the wavelengths used for measuring spike signals (705 nm), scattering did not lead to a large overestimate of cell size; but it did degrade the signal-to-noise ratio. Fig. 6 illustrates the results of similar experiments carried out on the salamander olfactory bulb (Orbach & Cohen, 1983). The top section indicates that, when no tissue is present, essentially all of the light (750 nm) from a small spot falls on



1. lamp housing 3. shutter 5. x-y stage 7. diode array
 2. filter holder 4. dichroic mirror 6. z 8. camera lens

Fig. 5. Photograph of a microscope constructed around a 25-mm, 0.95 f, C-mount camera lens. This lens is used to form a magnified image of the preparation onto the photodiode array. With this microscope, at a magnification of $4\times$, 100 times more light reached the photodetectors than with our conventional microscope. The end of the 25-mm lens that normally faces the camera is facing the preparation. This orientation results in a larger numerical aperture. The light source is a 12 V, 100 W, tungsten filament bulb. With the illumination intensities available with this system, photodynamic damage is seen after several 20-s periods of illumination in the experiments on turtle visual cortex; thus, the use of a brighter light source would be counterproductive for these recordings.

one detector. Fig. 6C illustrates the result when a 500- μm -thick slice of olfactory bulb is present. The light from the small spot is spread to about 200 μm . Mammalian cortex appears to scatter more than the olfactory bulb. Thus, light scattering will cause considerable blurring of signals in adult vertebrate preparations.

A second source of blurring is signal from regions that are out of focus. For example, if the active region is a cylinder (a column) perpendicular to the plane of focus and the objective is focused at the middle of the cylinder, then the light from the middle will have the correct diameter at the image plane. However, the light from the regions above and below are out of focus and will have a

diameter that is too large. Fig. 6B illustrates the effect of moving the small spot of light 500 μm out of focus. The light from the small spot is spread to about 200 μm . Thus, in preparations with considerable scattering or with out-of-focus signals, the actual spatial resolution may be limited by the preparation and not by the number of pixels in the imaging device.

Confocal and two-photon microscopes. The confocal microscope (Petran & Hadravsky (1966)) substantially reduces both the scattered and the out-of-focus light that contributes to the image. More recently, a modification using two-photon excitation of the fluorophore has been developed. This kind of

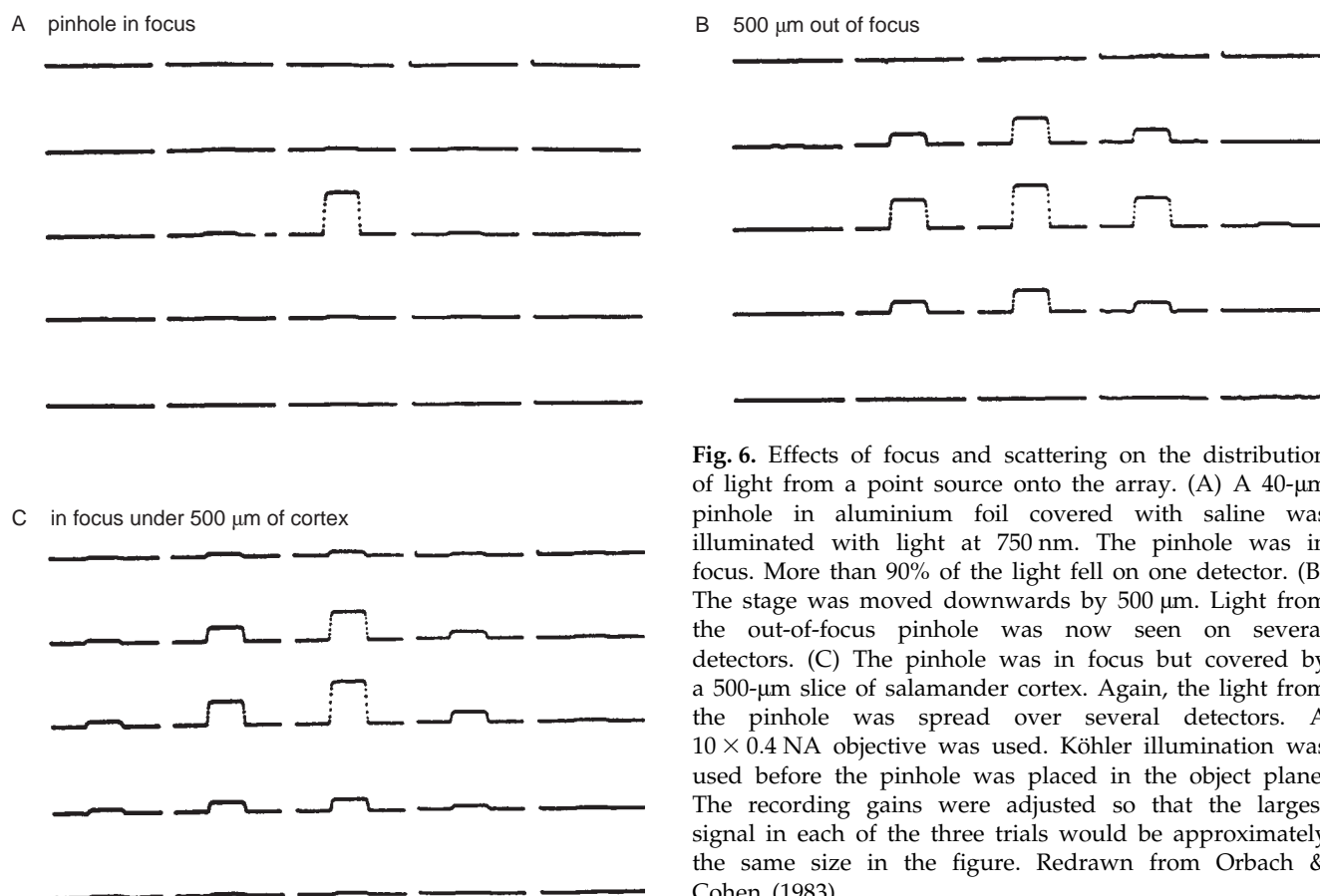


Fig. 6. Effects of focus and scattering on the distribution of light from a point source onto the array. (A) A 40- μm pinhole in aluminium foil covered with saline was illuminated with light at 750 nm. The pinhole was in focus. More than 90% of the light fell on one detector. (B) The stage was moved downwards by 500 μm . Light from the out-of-focus pinhole was now seen on several detectors. (C) The pinhole was in focus but covered by a 500- μm slice of salamander cortex. Again, the light from the pinhole was spread over several detectors. A 10×0.4 NA objective was used. Köhler illumination was used before the pinhole was placed in the object plane. The recording gains were adjusted so that the largest signal in each of the three trials would be approximately the same size in the figure. Redrawn from Orbach & Cohen (1983).

excitation reduces out-of-focus fluorescence and photobleaching (Denk *et al.*, 1995). With both types of microscope, one can obtain images from intact vertebrate preparations with much better spatial resolution than was achieved with ordinary microscopy. These microscopes have been used very successfully to monitor changes in calcium concentration inside small processes of neurons (Eilers *et al.*, 1995; Yuste & Denk, 1995). However, at present, the sensitivity of these microscopes is relatively poor; there are no reports of their use to measure the small signals obtained with voltage-sensitive dyes of the type discussed in this article. On the other hand, slower voltage-sensitive dye signals have been measured confocally (Loew, 1993).

Random-access fluorescence microscopy. Bullen *et al.* (1997) have used acousto-optic deflectors to construct a random-scanning microscope and were able to measure signals from parts of cultured hippo-

campal neurons. To reduce the effects of fluctuations in the laser output, the fluorescence signals were divided by the output of a photodetector sampling the incident light. Relatively large signal-to-noise ratios were obtained using voltage-sensitive dyes; however, there was no direct comparison with the signal-to-noise ratios obtained with a photodiode array system.

Photodetectors

As the signal-to-noise ratio in a shot noise-limited measurement is proportional to the square root of the number of photons converted into photoelectrons (see above), quantum efficiency is critical. As indicated in Table 1, silicon photodiodes have quantum efficiencies approaching the ideal at wavelengths at which most dyes absorb or emit light (500–900 nm). In contrast, only specially chosen vacuum photocathode devices (phototubes, photomultipliers or image in-

Table 1. Detector comparison

	Silicon diode	Vacuum photocathode
Quantum efficiency	0.9	0.15
Dark noise equivalent power	$\sim 10^7$ photons s^{-1}	$< 10^5$ photons s^{-1}
1/f noise	Some diodes	No

tensifiers) have a quantum efficiency as high as 0.15. Thus, in shot noise-limited situations, a silicon diode will have a signal-to-noise ratio that is at least 2.5 times larger. This advantage is indicated in Fig. 4 by the fact that the diode curve (solid line) is higher than the vacuum photocathode curve (dashed line) over much of the intensity range (segment B).

Dark noise can degrade the signal-to-noise ratio from this theoretical limit. While the dark noise is generally far larger in a silicon diode system than in a vacuum photocathode system (Table 1), the diode dark noise can be reduced substantially by cooling. Nonetheless, at low light levels (e.g. $<10^7$ photons ms^{-1} at room temperature), a vacuum photocathode device will provide a larger signal-to-noise ratio. When the light level is reduced so that the shot noise is less than the dark noise, the signal-to-noise ratio decreases linearly with light intensity (segment A, Fig. 4). The crossover in signal-to-noise ratio between the silicon diode and the vacuum photocathode device occurs at about 10^7 photons ms^{-1} at room temperature (arrow 1, Fig. 4), which is near the intensities obtained in fluorescence measurements from individual neurons stained with voltage-sensitive or ion-sensitive dyes. The fluorescence intensity from ganglia and intact cortex is large enough so that silicon photodiodes are optimal.

Imaging devices

Many factors must be considered in choosing an imaging system. Perhaps the most important considerations are the requirements for spatial and temporal resolution. Because the signal-to-noise ratio in a shot noise-limited measurement is proportional to the number of measured photons, increases in either temporal or spatial resolution reduce the signal-to-noise ratio. While several types of imaging devices will be considered, the emphasis will be on systems that allow frame rates near 1 kHz.

Film. One type of imager that has outstanding spatial and temporal resolution is movie film. But, because it is difficult to obtain quantum efficiencies of even 1% with film (Shaw, 1979), there would be a substantial degradation in signal-to-noise. This and other difficulties, including frame-to-frame and within-frame non-uniformity of the emulsion, has discouraged attempts to use film.

Silicon diode arrays. Arrays of silicon diodes are attractive because they have nearly ideal quantum efficiencies.

Parallel readout arrays. Diode arrays with 256–1020 elements are now in use in several laboratories (Iijima *et al.*, 1989; Nakashima *et al.*, 1992; Zecevic *et al.*, 1989; Hirota *et al.*, 1995). In addition, Hamamatsu has constructed a system with 2500 elements.

These arrays are designed for parallel readout; each detector is followed by its own amplifier whose output can be digitized at frame rates of 1 kHz. While the need to provide a separate amplifier for each diode element limits the number of pixels in parallel readout systems, it contributes to the very large (10^5) dynamic range that can be achieved. A discussion of amplifiers has been presented earlier (Wu & Cohen, 1993). Two parallel readout array systems are commercially available; items 3 and 4 in Approximate costs.

Serial readout arrays. By using serial readout, the number of amplifiers can be reduced. Gen Matsu-moto and his collaborators at the Electrotechnical Laboratory in Tsukuba City together with Fuji Film have implemented a 128×128 (16 384 pixel) CCD array that can be read out at a frame rate of 2 kHz (Ichikawa *et al.*, 1992; Iijima *et al.*, 1992). At 1 kHz, the data rate from this system is 32 Mbytes s^{-1} , requiring relatively specialized hardware for recording. The commercial Fuji system is much less sensitive than parallel readout arrays at the light levels obtained in fluorescence measurements from the nervous system. Furthermore, the Fuji system saturates at the light levels that can be obtained in absorption measurements and, therefore, must be used with reduced illumination (which reduces the signal-to-noise ratio). Several slower systems based on CCD cameras have been used to measure activity-dependent optical signals in neurobiological preparations (Lasser-Ross *et al.*, 1991; Delaney *et al.*, 1994; Poe *et al.*, 1994). Lasser-Ross *et al.* (1991) have modified the software for a Photometrics CCD camera to allow several choices of spatial and temporal resolution. Table 2, from their paper, illustrates these choices. The dynamic range of CCD cameras is limited by saturation and by the accuracy of the analogue-to-digital conversion. A dynamic range of 10^3 is not easily achieved. These cameras saturate at the fluorescence intensities that can be obtained from vertebrate brain preparations but are close to ideal for measurements from individual neurons stained with internally injected dyes.

Vacuum photocathode cameras. While the lower quantum efficiencies of vacuum photocathodes is a disadvantage, these devices may be preferable in low light measurements (Fig. 4). One of these, a Radechon

Table 2. Spatial and temporal resolution from a photometrics camera (from Lasser-Ross *et al.*, 1991)

Frame rate	Pixels
100 s^{-1}	324
40 s^{-1}	2 500
20 s^{-1}	10 000

(Kazan & Knoll, 1968), has an output proportional to the changes in the input. Vacuum photocathode cameras have been used in recordings from mammalian cortex (Blasdel & Salama, 1986) and salamander olfactory bulb (Kauer, 1988; Cinelli *et al.*, 1995).

In most of these systems, the image recorder has been placed in the objective image plane of a microscope. However, Tank and Ahmed (1985) suggested a scheme by which a hexagonal close-packed array of optical fibres is positioned in the image plane, and individual photodiodes are connected to the other end of the optical fibres. The 464-pixel cameras sold by OptImaging, LLC. (see Approximate costs) are based on this scheme.

Dynamic range

An important figure of merit for an optical recording system is dynamic range; this number can be specified in db, in bits, or as an exponent (e.g. 100 db = 17 bits = 10^5). The dynamic range determines the size of smallest fractional change that can be measured. For example, a dynamic range of 100 db would allow one to measure a signal with a fractional change ($\Delta I/I$) of 10^{-5} . The smallest signal that can be measured with a dynamic range of 60 db is 10^{-3} . The dynamic range cannot be larger than the effective resolution of the analogue-to-digital converter, but it can be considerably smaller if, for example, saturation in the photodetector limits the number of measured photons. Dynamic range can also be reduced by extraneous noise (see above).

Other optical signals

Improvements in the signal-to-noise ratios would clearly be useful. Only for absorption, fluorescence and birefringence have a large number of dyes been tested. A number of avenues remain partially or completely unexplored.

Gonzalez and Tsien (1995) measured energy transfer between a pair of dyes, one within the membrane and one on a lectin molecule bound to the outside of the membrane. In tissue culture preparations, they found fractional fluorescence changes (about 10%) that are as big as the largest signals found with styryl dyes in similar preparations (Grinvald *et al.*, 1982a; Loew *et al.*, 1985). One difficulty with the requirement that one of the pair be within the membrane is that it must be quite hydrophobic; hydrophobic dyes will be difficult to use in intact preparations, because they will not penetrate into the tissue. It is hoped that further efforts will remove this restriction and increase the size of the signal.

Bouevitch *et al.* (1993) and Ben-Oren *et al.* (1996) found that membrane potential changed the non-linear second harmonic generation from styryl dyes in cholesterol bilayers and in fly eyes. Large (50%)

fractional changes were measured. It is hoped that improvements in the illumination intensity will result in larger signal-to-noise ratios.

Ehrenberg and Berezin (1984) have used resonance Raman to study surface potential; these methods might also be applicable for measuring transmembrane potential. There was a report of holographic signals in leech neurons (Sharnoff *et al.*, 1978a), but signals were not found in subsequent experiments on squid axons (Sharnoff *et al.*, 1978b). There were also reports of changes in intrinsic infrared absorption (Sherebrin, 1972; Sherebrin *et al.*, 1972), but these have not been pursued further.

Two examples

Action potentials from individual neurons in an Aplysia ganglion

Nervous systems are made up of large numbers of neurons; and many of these are simultaneously active during the generation of behaviours. The original motivation for developing optical methods was the hope that they could be used to record all of the action potential activity of all the neurons in simpler invertebrate ganglia during behaviours (Davila *et al.*, 1973). Techniques that use microelectrodes to monitor activity are limited in that they can observe single cell activity in only as many cells as one can simultaneously place electrodes (typically two or three neurons). Obtaining information about the activity of many cells is essential for understanding the roles of the individual neurons in generating behaviour and for understanding how nervous systems are organized.

In the first attempt to use voltage-sensitive dyes in ganglia (Salzberg *et al.*, 1973), we were fortunate to be able to monitor activity in a single neuron, because the photodynamic damage was severe and the signal-to-noise ratio small. Now, however, with better dyes and methods, the spike activity of hundreds of individual neurons can be recorded simultaneously (Zecevic *et al.*, 1989; Nakashima *et al.*, 1992). In the experiments described below, we measured the spike activity of up to 50% of the approximately 1000 cells (Cash & Carew, 1989; Coggeshall, 1967) in the *Aplysia* abdominal ganglion. Opisthobranch molluscs have been a preparation of choice for this kind of measurement, because their central nervous systems have relatively few, relatively large neurons and almost all of the cell bodies are fully invaded by the action potential. This is important because the signal-to-noise ratio for action potential recording in ganglia is not large, and it would be even lower if the cell bodies did not have a full-sized action potential.

Optical recordings were made using a 464-element

silicon photodiode array system with parallel readout (Fig. 7) (Falk *et al.*, 1993; Wu & Cohen, 1993). The diode array was placed in the image plane formed by a microscope objective of 25×0.4 na. A single-pole highpass and a four-pole lowpass Bessel filter in the amplifiers limited the frequency response to 1.5–200 Hz. We used the isolated siphon preparation developed by Kupfermann *et al.* (1971). Considerable effort was made to find conditions that maximized the dye staining while causing minimal pharmacological effects on the gill-withdrawal behaviour. Intact ganglia were incubated in a 0.15 mg ml^{-1} solution of the oxonol dye, RH155 (Fig. 1) (or its diethyl analogue) using a protocol developed by Nakashima

et al. (1992). A light mechanical stimulation (1–2 g) was delivered to the siphon.

Because the image of a ganglion is formed on a rectilinear diode array, there is no simple correspondence between images of cells and photodetectors (Fig. 7, lower right). The light from larger cell bodies will fall on several detectors, and its activity will be recorded as simultaneous events on neighbouring detectors. In addition, because these preparations are multilayered, most detectors will receive light from several cells. Thus, a sorting step is required to determine the activity in neurons from the spike signals on individual photodiodes. In the top right of Fig. 8 the raw data from seven

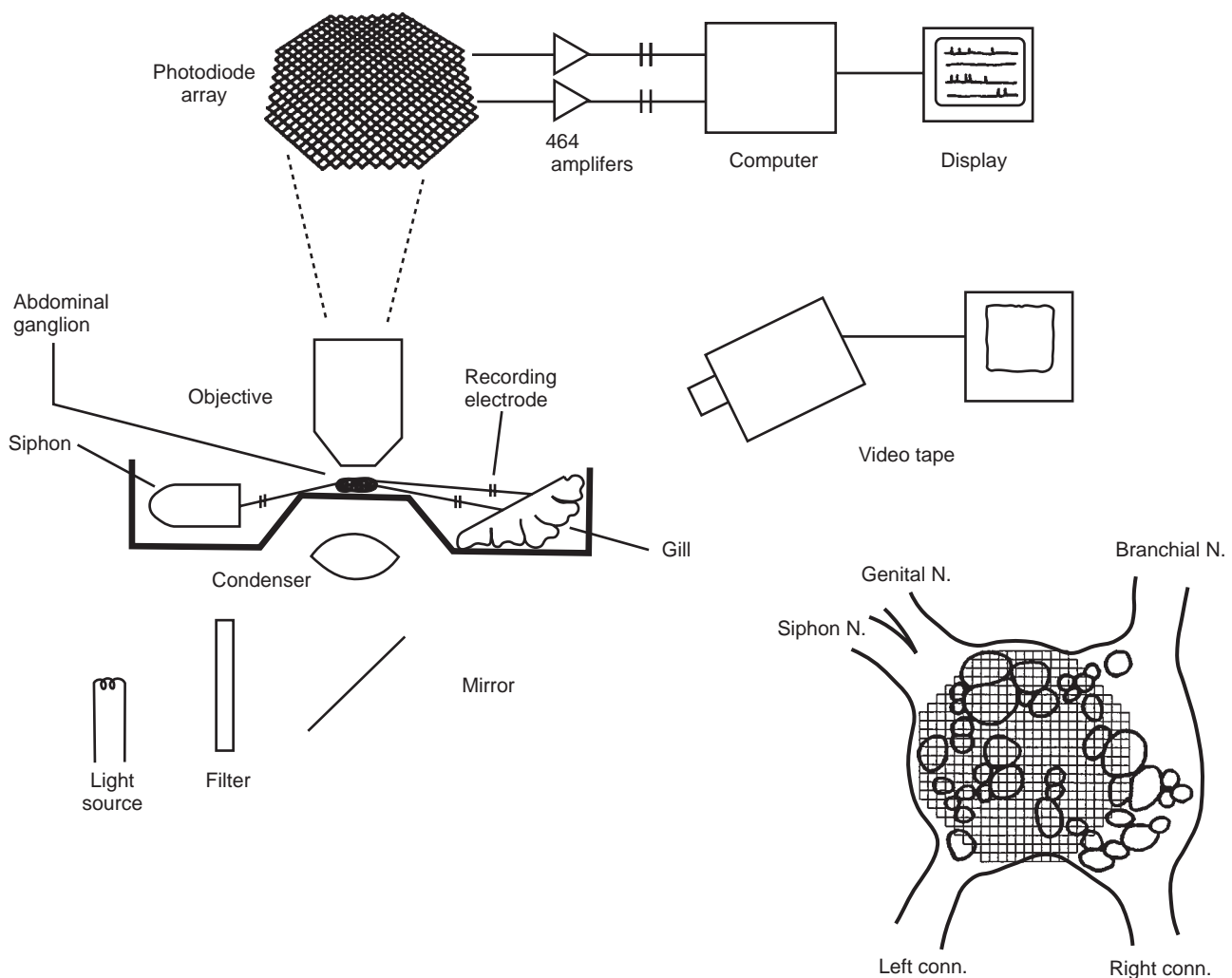


Fig. 7. Schematic diagram of the apparatus used in the *Aplysia* measurements. Light from a tungsten halogen lamp passed through a 720 ± 25 nm interference filter and was focused on the preparation. We used a modification of Köhler illumination (Leitz Ortholux II microscope) where the condenser iris was opened so that the condenser numerical aperture would equal the objective numerical aperture. A 464-element photodiode array was placed at the plane where the objective forms the real, inverted image. The outputs from each diode were amplified individually. The amplifier outputs were digitized by a 512-channel, 12-bit, analogue-to-digital converter and stored in a PC computer. The figure illustrates the isolated siphon preparation (Kupfermann *et al.*, 1971). The relative size and position of the photodiode array and the image of an *Aplysia* abdominal ganglion is shown on the lower right. Redrawn from Falk *et al.* (1993).

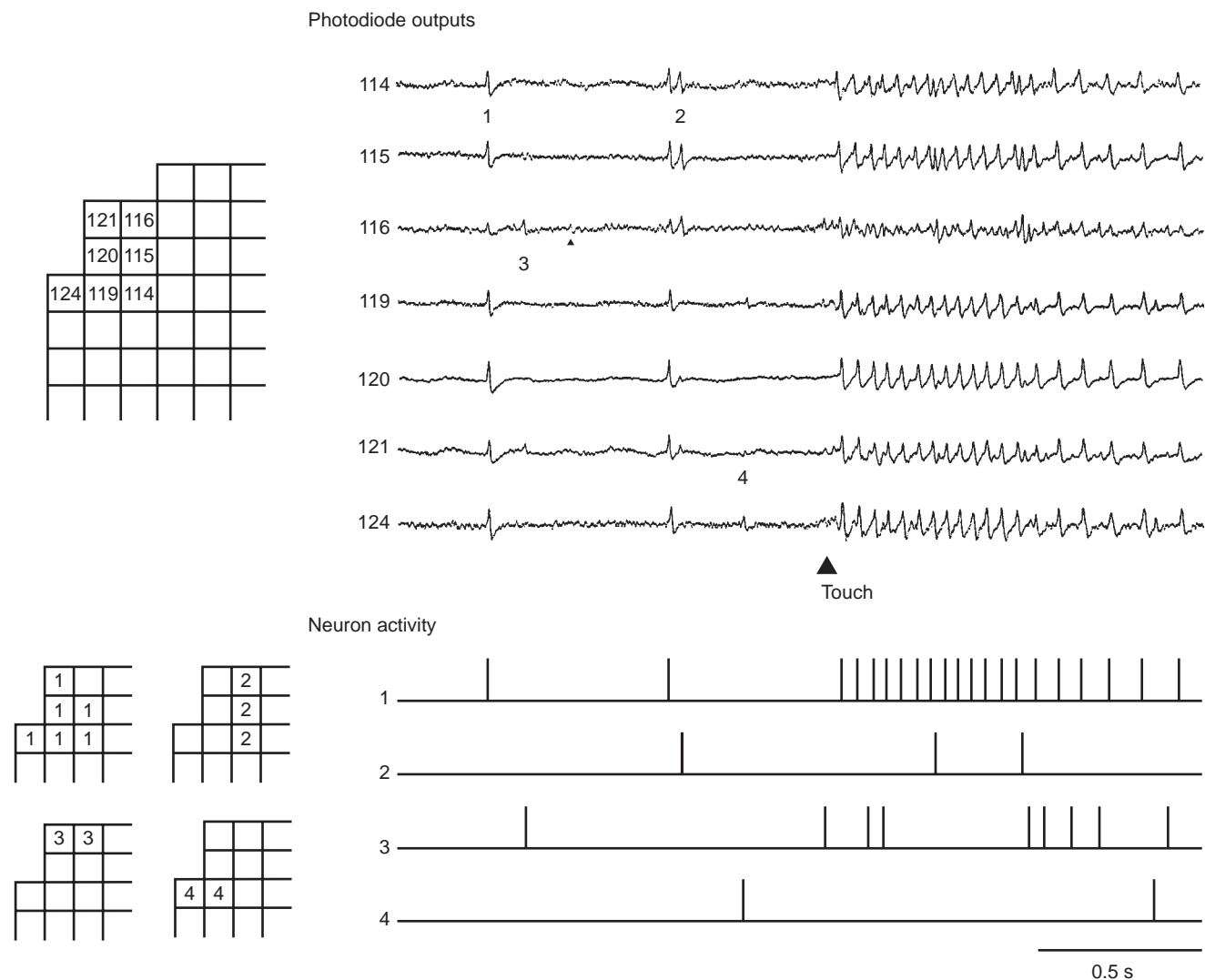


Fig. 8. Optical recordings from a portion of a photodiode array from an *Aplysia* abdominal ganglion. The drawing to the left represents the relative position of the detectors whose activity is displayed. In the top right, the original data from seven detectors is illustrated. The numbers to the right of each trace identify the detector from which the trace was taken. The bottom section shows the raster diagram illustrating the results of our sorting of this data into the spike activity of four neurons. At the number 1 in the top section, there are synchronously occurring spike signals on all seven detectors. A synchronous event of this kind occurs more than 20 times; we presume that each event represents an action potential in one relatively large neuron. The activity of this cell is represented by the vertical lines on trace 1 of the bottom section. The activity of a second cell is indicated by small signals at the number 4 on 119 and its neighbour, 124. The activity of this cell is represented by the vertical lines on trace 4 of the bottom section. The activity of neurons 2 and 3 was similarly identified. Modified from Zecevic *et al.*, (1989).

photodiodes from an array are shown. The activity of four neurons (shown in the raster diagram at the bottom) can account for the spike signals in the top section. Two problems are illustrated in this figure. Both arise from the signal-to-noise ratio. First, there may be an additional spike on detector 116 just before the stimulus (at the arrow), but the signal-to-noise ratio was not large enough to be certain. Secondly, following the stimulus, there is a great deal of activity that will obscure small signals.

The result of a complete analysis is shown in the

raster diagram of Fig. 9. The mechanical stimulus occurred at the time indicated by the bar at the bottom. There are 135 neurons whose activity was detected optically. Similar results have been obtained by Nakashima *et al.* (1992). We estimated that the recording illustrated in Fig. 9 was about 50% complete (Wu *et al.*, 1994b). Thus, the actual number of activated neurons during the gill-withdrawal reflex was about 300.

We were surprised at the large number of neurons that were activated by the light touch.

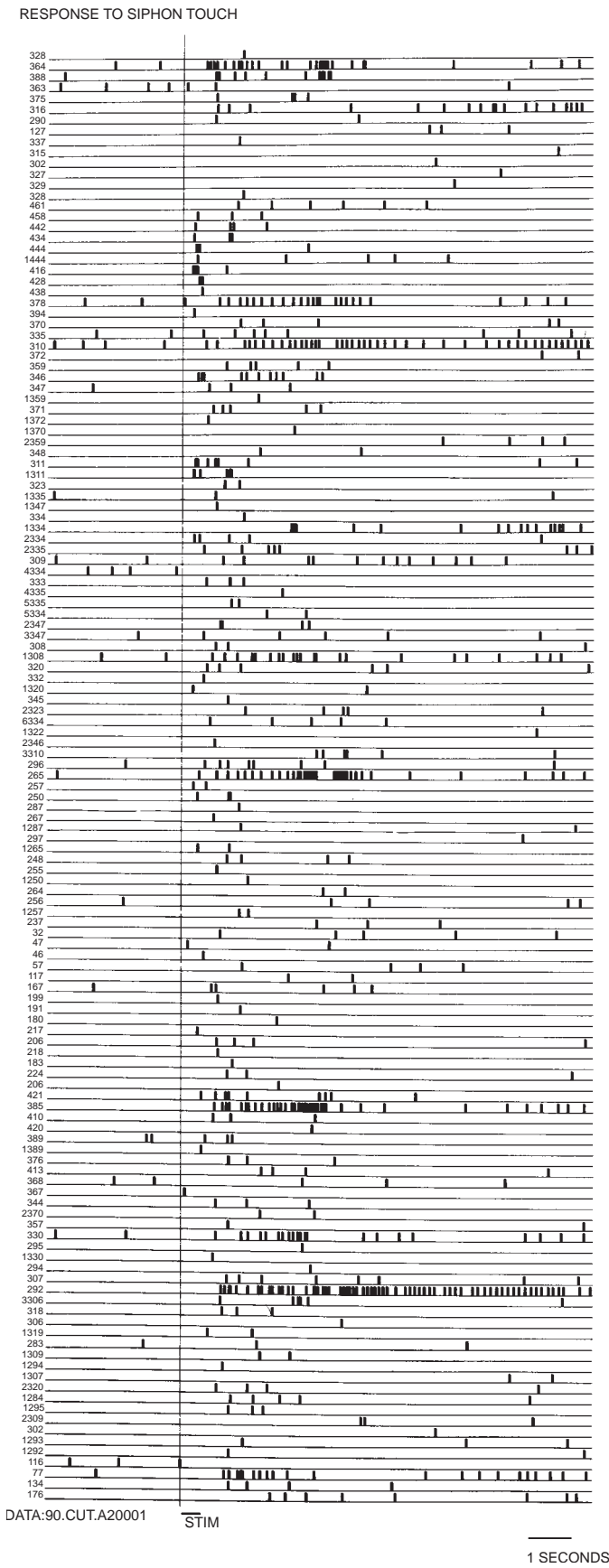


Fig. 9. Raster diagram of the action potential activity recorded optically from an *Aplysia* abdominal ganglion during a gill-withdrawal reflex. The touch to the siphon occurred at the time of the bar labelled STIM. In this recording, activity in 135 neurons was measured. We think this recording is incomplete and that the actual number of active neurons was between 250 and 300. Most neurons are activated by the touch but one, no. 4334 (about 1/3 down from the top), was inhibited. This inhibition was seen in repeated trials in this preparation. Modified from Wu *et al.* (1994b).

Furthermore, a substantial number of the remaining neurons are likely to be either inhibited by the stimulus or receive a large subthreshold excitatory input. It is almost as if the *Aplysia* nervous system is designed such that every cell in the abdominal ganglion cares about this (and perhaps every) sensory stimulus. In addition, more than 1000 neurons in other ganglia are activated by this touch (Tsau *et al.*, 1994). Clearly information about this very mild and localized stimulus is propagated widely in the *Aplysia* nervous system. These results force a more pessimistic view of the present understanding of the neuronal basis of apparently simple behaviours in relatively simple nervous systems. Elsewhere, we present arguments suggesting that the abdominal ganglion may function as a distributed system (Wu *et al.*, 1994; Tsau *et al.*, 1994).

Population signals from turtle visual cortex

In the preceding experiments on *Aplysia* ganglia, each detector received light from one neuron or a small number of neurons. In contrast, in measurements from the turtle visual cortex, each detector received light from a 200- μm square area of cortex, which includes thousands of neurons. The resulting signal will be a population average of the change in membrane potential of all of these cells. Populations signals have been recorded from many preparations (e.g. Grinvald *et al.*, 1982b; Orbach & Cohen, 1983; Sakai *et al.*, 1985; Kauer, 1988; Cinelli & Salzberg, 1992; Albowitz & Kuhnt, 1993); the results from

turtle are described because of our familiarity with them.

Prechtl (1994) discovered that visual stimuli induced oscillations in the local field potential of the turtle visual cortex. He found that a moving stimulus would induce oscillations that were sometimes synchronous when comparing regions of dorsal cortex and the dorsal ventricular ridge. This synchrony at two locations would imply that there was a standing wave of depolarization. We measured the voltage-sensitive dye signal that accompanies these oscillations; this allowed a detailed visualization of their spatiotemporal characteristics.

The dorsal cortex was exposed by removing the overlying bone; the pial surface was incubated with a 0.25–0.8 mg ml^{-1} solution of the styryl dyes, RH-795 (Grinvald *et al.*, 1994) or JPW1114 (Antic & Zecevic, 1995) for 15 min. No other dyes were tested. The brain was partially isolated by sectioning the spinal cord and cutting cranial nerves IV–XII. To eliminate artifacts resulting from the heartbeat and the movement of blood cells through the brain, the turtle was perfused with a steady flow of an oxygenated artificial cerebrospinal fluid.

Two kinds of stimuli were used: a step increase in diffuse light or a looming stimulus; both had a duration of 3 s. Fig. 10A (Prechtl *et al.*, 1997) shows the responses from a single photodetector to both a looming (top) and a diffuse light (bottom) stimulus. The diode output was filtered with a bandpass of 0.35–50 Hz. For both stimuli, part of the response is a relatively large and long-lasting depolarization.

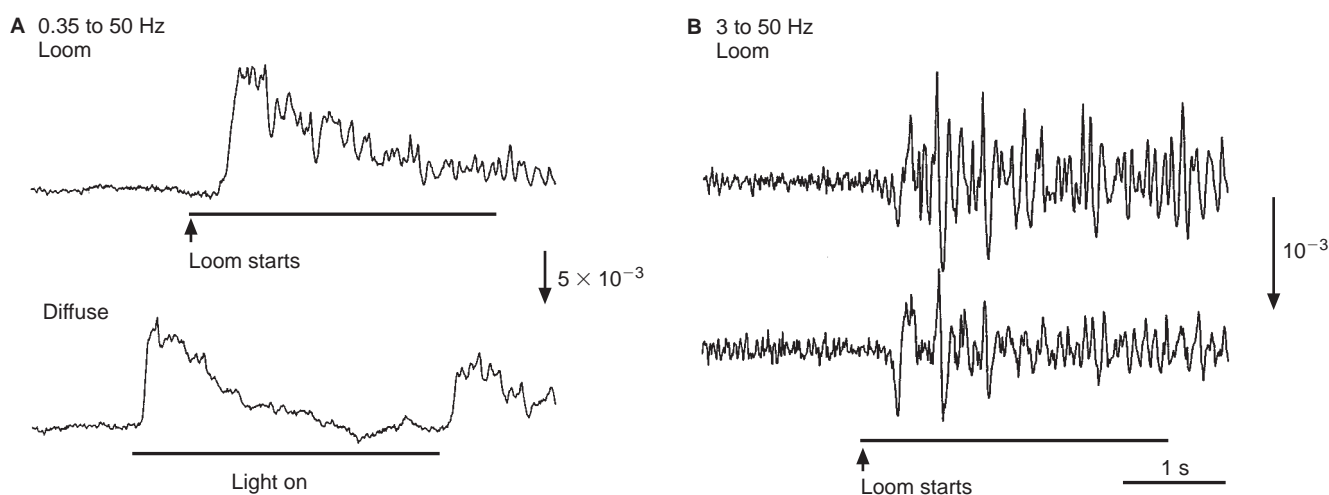


Fig. 10. The outputs of individual detectors in a population signal measurement from turtle visual cortex. The responses to both looming and diffuse light stimuli include both very low frequency (<0.1 Hz) and higher frequency (1–30 Hz) components. (A) The response of the same detector to the two kinds of visual stimuli. (B) The response to a looming stimulus measured simultaneously in two different detectors. To emphasize the high-frequency components, these signals have been further filtered to remove components below 3 Hz. The length of the vertical calibration on the right represents the stated value of the change in fluorescence divided by the resting fluorescence ($\Delta F/F$). Modified from Prechtl *et al.* (1997).

The response to the looming stimulus has a longer latency and returned to the baseline more slowly. From the signals measured with the same dyes on other preparations where there was a direct comparison with an intracellular electrode recording, we infer that an upward deflection in this figure represents a depolarization.

Riding on top of the long-lasting components in Fig. 10A are higher frequency signals; these were larger in the looming response than in the diffuse light response. These high-frequency components are emphasized by increasing the high-pass cutoff to 3.0 Hz and increasing the gain (Fig. 10B). The top trace in Fig. 10B is from the same data as that shown in the top trace in Fig. 10A. The bottom trace in Fig. 10B is from a second detector, which received light from an area of cortex that was 1.2 mm away. Although a few events in these two detectors appear to be in phase, there are many instances where the two traces are quite different. This result implies that the high-frequency signal does not result from either a simple standing wave or a repetitive travelling wave. It is, however, very difficult to infer anything about the spatial spread of these signals from an examination of these two traces.

The same experiment is presented as a series of pseudocolour frames made using the data from all of the diode array (Fig. 11). Each frame is separated by 4 ms; red represents depolarizations and purple hyperpolarizations (normalized to each detector). The series starts at the top left and goes left-to-right and then top-to-bottom. The time of the beginning of the looming stimulus is 684 ms before the first picture. The response consists of a very complex, non-repeating pattern of travelling and/or expanding and contracting waves of depolarization that continues after the end of the stimulus. The waves differ in their origins, direction and speed of travel, end points and the area of cortex involved (Prechtl *et al.*, 1997).

Thus, the voltage-sensitive dye recording has provided a uniquely detailed picture of the spatial aspects of this oscillatory response. This response is quite complex and, indeed, more complex than Prechtl (1994) had anticipated from his local field potential measurements.

In vivo mammalian brain

Measuring population signals from *in vivo* mammalian preparations is more difficult than the perfused turtle because of additional sources of noise from the heartbeat and respiration and probably also because mammalian preparations are not as easily stained. Two methods for reducing the movement artifacts from the heartbeat are, together, quite effective. First, a subtraction procedure is used where two record-

ings are made but only one of the trials has a stimulus (Orbach *et al.*, 1985). Both recordings are triggered from the upstroke of the electrocardiogram so both should have similar heartbeat noise. When the trial without the stimulus is subtracted from the trial with the stimulus the heartbeat artifact is reduced. Secondly, an airtight chamber is fixed onto the skull surrounding the craniotomy (Blasdel & Salama, 1986). When this chamber is filled with silicon oil and closed, the movements caused by heartbeat and respiration are substantially reduced. Using both methods reduces the noise from these movement artifacts enough, so that it is no longer the main source of noise in the measurement.

Future directions

Attempts to measure the action potential activity in many neurons during behaviours has been carried out in only two situations, the gill-withdrawal reflex in *Aplysia* and feeding in *Navanax* (London *et al.*, 1987). Similarly, optical recordings from vertebrate brain during behaviours have been made in only a few instances. Thus, an obvious future direction is to apply these techniques to other behaviours and preparations.

A second direction is to improve the sensitivity of the voltage-sensitive dye measurements. Because the apparatus is already optimized, much of this improvement will need to come from the development of better dyes and investigating signals from additional optical properties of the dyes.

A third direction is the development of methods for neuron type-specific staining of vertebrate preparations. The use of retrograde staining procedures has recently been investigated in the embryonic chick and lamprey spinal cords (Hickie *et al.*, 1996; Tsau *et al.*, 1996; Wenner *et al.*, 1996). Spike signals from individual neurons were measured in the lamprey experiments. An identified cells class (motoneurons) was selectively stained. Further efforts at optimizing this staining procedure are needed. A second possibility is the use of cell type-specific staining developed for fluorescein by Nirenberg and Cepko (1993). It might be possible to use similar techniques for voltage-sensitive or ion-sensitive dyes. Third, Siegel & Isacoff (1997) constructed a genetically encoded combination of a potassium channel and green fluorescent protein. When introduced into a frog oocyte, this molecule had a (relatively slow) voltage-dependent signal with a fractional fluorescence change of 5%.

Optical recordings provide unique insights into brain activity and organization. Improvements in sensitivity or selectivity would make these methods more powerful.

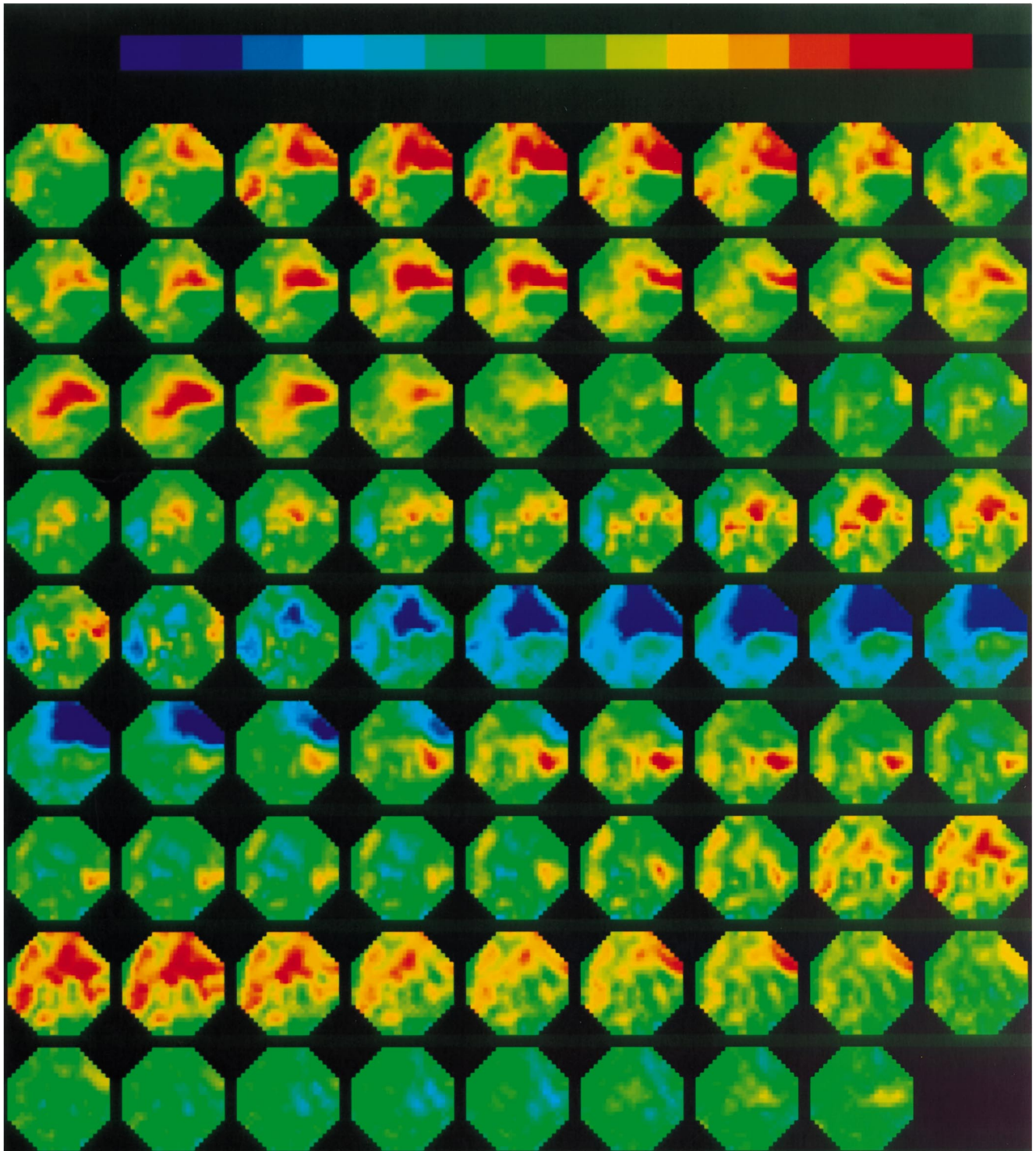


Fig. 11. Pseudocolour images of turtle visual cortex in response to a looming stimulus. The depolarizing events are both complex and variable. The data were filtered with a bandpass of 3–50 Hz (as in Fig. 10B) before making the display. Frames were recorded every millisecond but each frame in this figure has the average intensity for a 4-ms period. The first frame (upper left corner) occurs 684-ms before the onset of the stimulus. The last frame (bottom right corner) is 320-ms later. The pseudocolour pictures from the period after the stimulus were similar to the frames shown in the bottom line of this figure. The pseudocolour pictures were made by assigning red to depolarizations and purple to hyperpolarizations. Modified from Prechtl *et al.* (1997).

Approximate costs (in the US: \$US, November 1996)

- | | |
|---|--------|
| 1. 250-W Xenon arc lamp housing and power supply Opti-Quip, Highland Mills, NY, USA | 4000 |
| 2. Microscope illustrated in Fig. 5 | |
| a. Stand (Spindler & Hoyer, Milford, MA, USA) | 100 |
| b. Sliders (Spindler & Hoyer) | 800 |
| c. X-Y stage (New England Applied Technologies, Lawrence, MA, USA) | 600 |
| d. Lens; precision 25 mm 0.95 f, C-mount lens | 300 |
| e. Dichroic mirror (Omega Optical, Brattleboro, VT, USA) | 150 |
| f. Mirror and lens holders (Spindler & Hoyer) | 600 |
| 3. 464-element photodiode array system | 70 000 |
| Diode array, housing, first and second stage amplifiers, a-to-d converter, computer, software (OptImaging, LLC, Fairfield, CT, USA) | |
| 4. 256-element photodiode array system. | 14 000 |
| Diode array and first-stage amplifier (Hamamatsu Corp. Bridgewater, NJ, USA) | |

Acknowledgements

The authors are indebted to their collaborators Vicencio Davila, Amiram Grinvald, Kohtaro Kamino, Bill Ross, Brian Salzberg, Alan Waggoner and Joe Wuskell for numerous discussions about optical methods. The experiments carried out in our laboratories were supported by NIH grants NS08437 and GM35063.

References

- ALBOWITZ, B. & KUHN, U. (1993) Spread of epileptiform potentials in the neocortical slice: recordings with voltage-sensitive dyes. *Brain Res.* **631**, 329–33.
- ANTIC, S. & ZECEVIC, D. (1995) Optical signals from neurons with internally applied voltage-sensitive dyes. *J. Neurosci.* **15**, 1392–405.
- BEN-OREN, I., PELEG, G., LEWIS, A., MINKE, B. & LOEW, L. (1996) Infrared nonlinear optical measurements of membrane potential in photoreceptor cells. *Biophys. J.* **71**, 1616–20.
- BLASDEL, G.G. & SALAMA, G. (1986) Voltage-sensitive dyes reveal a modular organization in monkey striate cortex. *Nature* **321**, 579–85.
- BOUEVITCH, O., LEWIS, A., PINEVSKY, I., WUSKELL, J. & LOEW, L. (1993) Probing membrane potential with nonlinear optics. *Biophys. J.* **65**, 672–9.
- BOYLE, M.B. & COHEN, L.B. (1980) Birefringence signals that monitor membrane potential in cell bodies of molluscan neurons. *Fed. Proc.* **39**, 2130.
- BRADDICK, H.J.J. (1960) Photoelectric photometry. *Rep. Prog. Phys.* **23**, 154–75.
- BULLEN, A., PATEL, S.S. & SAGGAU, P. (1997) High-speed, random-access fluorescence microscopy: I. High resolution optical recording with voltage-sensitive dyes and ion indicators. *Biophys. J.* **73**, 477–91.
- CASH, D. & CAREW, T.J. (1989) A quantitative analysis of the development of the central nervous system in juvenile *Aplysia californica*. *J. Neurobiol.* **20**, 25–47.
- CINELLI, A.R. & SALZBERG, B.M. (1992) Dendritic origin of late events in optical recordings from salamander olfactory bulb. *J. Neurophysiol.* **68**, 786–806.
- CINELLI, A.R., NEFF, S.R. & KAUER, J.S. (1995) Salamander olfactory bulb neuronal activity observed by video rate, voltage-sensitive dye imaging. I. Characterization of the recording system. *J. Neurophysiol.* **73**, 2017–32.
- COGGESHALL, R.E. (1967) A light and electron microscope study of the abdominal ganglion of *Aplysia californica*. *J. Neurophysiol.* **30**, 1263–87.
- COHEN, L.B. & LESHER, S. (1986) Optical monitoring of membrane potential: methods of multisite optical measurement. *Soc. Gen. Physiol. Ser.* **40**, 71–99.
- COHEN, L.B. & SALZBERG, B.M. (1978) Optical measurement of membrane potential. *Rev. Physiol. Biochem. Pharmacol.* **83**, 35–88.
- DELANEY, K.R., GELPERIN, A., FEE, M.S., FLORES, J.A., GERVAIS, R., TANK, D.W. & KLEINFELD, D. (1994) Waves and stimulus-modulated dynamics in an oscillating olfactory network. *Proc. Natl. Acad. Sci. USA* **91**, 669–73.
- DAINTY, J.C. (1984) *Laser Speckle and Related Phenomena*. New York: Springer-Verlag.
- DAVILA, H.V., SALZBERG, B.M., COHEN, L.B. & WAGGONER, A.S. (1973) A large change in axon fluorescence that provides a promising method for measuring membrane potential. *Nature New Biol.* **241**, 159–60.
- DENK, W., PISTON, D.W. & WEBB, W. (1995) Two-photon molecular excitation in laser-scanning microscopy. In *Handbook of Biological Confocal Microscopy* (edited by Pawley, J.W.) pp. 445–58. New York: Plenum Press.
- EHRENBERG, B. & BEREZIN, Y. (1984) Surface potential on purple membranes and its sidedness studied by resonance Raman dye probe. *Biophys. J.* **45**, 663–70.
- EILERS, J., CALLAWAERT, G., ARMSTRONG, C. & KONNERTH, A. (1995) Calcium signaling in a narrow somatic submembrane shell during synaptic activity in cerebellar Purkinje neurons. *Proc. Natl. Acad. Sci. USA*, **92**, 10272–6.
- FALK, C.X., WU JY, COHEN, L.B. & TANG, C. (1993) Non-uniform expression of habituation in the activity of distinct classes of neurons in the *Aplysia* abdominal ganglion. *J. Neurosci.* **13**, 4072–81.
- FROMHERZ, P., DAMBACHER, K.H., EPHARDT, H., LAMBACHER, A., MULLER, C.O., NEIGL, R., SCHADEN, H., SCHENK, O. & VETTER, T. (1991) Fluorescent dyes as probes of voltage transients in neuron membranes: Progress report. *Ber. Bunsenges. Phys. Chem.* **95**, 1333–45.
- GONZALEZ, J.E. & TSIEN, R.Y. (1995) Voltage sensing by fluorescence energy transfer in single cells. *Biophys. J.* **69**, 1272–80.
- GRINVALD, A. & FARBER, I.C. (1981) Optical recording of calcium action potentials from growth cones of

- cultured neurons with a laser microbeam. *Science* **212**, 1164–7.
- GRINVALD, A., ROSS, W.N. & FARBER, I. (1981) Simultaneous optical measurements of electrical activity from multiple sites on processes of cultured neurons. *Proc. Natl. Acad. Sci. USA* **78**, 3245–9.
- GRINVALD, A., HILDESHEIM, R., FARBER, I.C. & ANGLISTER, L. (1982a) Improved fluorescent probes for the measurement of rapid changes in membrane potential. *Biophys. J.* **39**, 301–8.
- GRINVALD, A., MANKER, A. & SEGAL, M. (1982b) Visualization of the spread of electrical activity in rat hippocampal slices by voltage-sensitive optical probes. *J. Physiol.* **333**, 269–91.
- GRINVALD, A., LIEKE, E., FROSTIG, R.D., GILBERT, C.D. & WIESEL, T.N. (1986) Functional architecture of cortex revealed by optical imaging of intrinsic signals. *Nature* **324**, 361–4.
- GRINVALD, A., FROSTIG, R.D., LIEKE, E. & HILDESHEIM, R. (1988) Optical imaging of neuronal activity. *Physiol. Rev.* **68**, 1285–366.
- GRINVALD, A., LIEKE, E.E., FROSTIG, R.D. & HILDESHEIM, R. (1994) Cortical point-spread function and long-range lateral interactions revealed by real-time optical imaging of macaque monkey primary visual cortex. *J. Neurosci.* **14**, 2545–68.
- GROSS, E., BEDLACK, R.S. & LOEW, L.M. (1994) Dual-wavelength ratiometric fluorescence measurements of the membrane dipole potential. *Biophys. J.* **67**, 208–16.
- GUPTA, R.K., SALZBERG, B.M., GRINVALD, A., COHEN, L.B., KAMINO, K., LESHER, S., BOYLE, M.B., WAGGONER, A.S. & WANG, C.H. (1981) Improvements in optical methods for measuring rapid changes in membrane potential. *J. Membr. Biol.* **58**, 123–37.
- HAMER, F.M. (1964) *The Cyanine Dyes and Related Compounds*. New York: Wiley.
- HICKIE, C., WENNER, P., O'DONOVAN, M., TSAU, Y., FANG, J. & COHEN, L.B. (1996) Optical monitoring of activity from individual and identified populations of neurons retrogradely labeled with voltage-sensitive dyes. *Abs. Soc. Neurosci.* **22**, 321.
- HIROTA, A., SATO, K., MOMOSE-SATO, Y., SAKAI, T. & KAMINO, K. (1995) A new simultaneous 1020-site optical recording system for monitoring neural activity using voltage-sensitive dyes. *J. Neurosci. Methods* **56**, 187–94.
- ICHIKAWA, M., IJIMA, T. & MATSUMOTO, G. (1992) *Simultaneous 16,384-site Optical Recording of Neural Activities in the Brain*. New York: Oxford University Press.
- IJIMA, T., ICHIKAWA, M. & MATSUMOTO, G. (1989) Optical monitoring of LTP and related phenomena. *Abstracts Soc. Neurosci.* **15**, 398.
- IJIMA, T., ICHIKAWA, M. & MATSUMOTO, G. (1992) Synaptic activation of rat adrenal medulla examined with a large photodiode array in combination with a voltage-sensitive dye. *Neuroscience* **51**, 211–19.
- KAUER, J.S. (1988) Real-time imaging of evoked activity in local circuits of the salamander olfactory bulb. *Nature* **331**, 166–8.
- KAZAN, B. & KNOLL, M. (1968) *Electronic Image Storage*. New York: Academic Press.
- KLEINFELD, D. & DELANEY, K.R. (1996) Distributed representation of vibrissa movement in the upper layers of somatosensory cortex revealed with voltage-sensitive dyes. *J. Comp. Neurol.* **375**, 89–108.
- KUPFERMANN, I., PINSKER, H., CASTELLUCCI, V. & KANDEL, E.R. (1971) Central and peripheral control of gill movements in *Aplysia*. *Science* **174**, 1252–6.
- LASSER-ROSS, N., MIYAKAWA, H., LEV-RAM, V., YOUNG, S.R. & ROSS, W.N. (1991) High time resolution fluorescence imaging with a CCD camera. *J. Neurosci. Methods* **36**, 253–61.
- LOEW, L.M. (1993) Confocal microscopy of potentiometric fluorescent dyes. *Methods Cell Biol.* **38**, 195–209.
- LOEW, L.M., COHEN, L.B., SALZBERG, B.M., OBAID, A.L. & BEZANILLA, F. (1985) Charge-shift probes of membrane potential. Characterization of aminostyrylpyridinium dyes on the squid giant axon. *Biophys. J.* **47**, 71–7.
- LONDON, J.A., ZECEVIC, D. & COHEN, L.B. (1987) Simultaneous optical recording of activity from many neurons during feeding in *Navanax*. *J. Neurosci.* **7**, 649–61.
- MALMSTADT, H.V., ENKE, C.G., CROUCH, S.R. & HARLICK, G. (1974) *Electronic Measurements for Scientists*. Menlo Park, CA: Benjamin.
- MOMOSE-SATO, Y., SATO, K., SAKAI, T., HIROTA, A., MATSUTANI, K. & KAMINO, K. (1995) Evaluation of optimal voltage-sensitive dyes for optical measurement of embryonic neural activity. *J. Membr. Biol.* **144**, 167–76.
- MORTON, D.W., CHIEL, H.J., COHEN, L.B. & WU, J.Y. (1991) Optical methods can be utilized to map the location and activity of putative motor neurons and interneurons during rhythmic patterns of activity in the buccal ganglion of *Aplysia*. *Brain Res.* **564**, 45–55.
- NAKASHIMA, M., YAMADA, S., SHIONO, S., MAEDA, M. & SATO, F. (1992) 448-detector optical recording system: development and application to *Aplysia* gill-withdrawal reflex. *IEEE Trans. Biomed. Eng.* **39**, 26–36.
- NIRENBERG, S. & CEPKO, C. (1993) Targeted ablation of diverse cell classes in the nervous system *in vivo*. *J. Neurosci.* **13**, 3238–51.
- ORBACH, H.S. & COHEN, L.B. (1983) Optical monitoring of activity from many areas of the *in vitro* and *in vivo* salamander olfactory bulb: a new method for studying functional organization in the vertebrate central nervous system. *J. Neurosci.* **3**, 2251–62.
- ORBACH, H.S., COHEN, L.B. & GRINVALD, A. (1985) Optical mapping of electrical activity in rat somatosensory and visual cortex. *J. Neurosci.* **5**, 1886–895.
- PETRAN, M. & HADRAVSKY, M. (1966) Czechoslovakian patent 7720.
- POE, G.R., RECTOR, D.M. & HARPER, R.M. (1994) Hippocampal retracted optical patterns during sleep and waking states in the freely behaving cat. *J. Neurosci.* **14**, 2933–42.
- PRECHTL, J.C. (1994) Visual motion induces synchronous oscillations in turtle visual cortex. *Proc. Natl. Acad. Sci. USA* **91**, 12467–71.
- PRECHTL, J.C., COHEN, L.B., PESERAN, B., MITRA, P.P. & KLEINFELD, D. (1997) Visual stimuli induce waves of electrical activity in turtle cortex. *Proc. Natl. Acad. Sci. USA* **94**, 7621–26.

- RATZLAFF, E.H. & GRINVALD, A. (1991) A tandem-lens epifluorescence microscope: hundred-fold brightness advantage for wide-field imaging. *J. Neurosci. Methods* **36**, 127–37.
- ROSS, W.N. & REICHARDT, L.F. (1979) Species-specific effects on the optical signals of voltage-sensitive dyes. *J. Membr. Biol.* **48**, 343–56.
- ROSS, W.N., SALZBERG, B.M., COHEN, L.B. & DAVILA, H.V. (1974) A large change in dye absorption during the action potential. *Biophys. J.* **14**, 983–6.
- SAKAI, T., HIROTA, A., KOMURO, H., FUJII, S. & KAMINO, K. (1985) Optical recording of membrane potential responses from early embryonic chick ganglia using voltage-sensitive dyes. *Brain Res.* **349**, 39–51.
- SALAMA, G. (1988) Voltage-sensitive dyes and imaging techniques reveal new patterns of electrical activity in heart and cortex. *SPIE Proc.* **94**, 75–86.
- SALZBERG, B.M. (1983) Optical recording of electrical activity in neurons using molecular probes. In *Current Methods in Cellular Neurobiology* (edited by BARKER, J.L. and MCKELVY, J.F.) pp. 139–87. New York: Wiley.
- SALZBERG, B.M., DAVILA, H.V. & COHEN, L.B. (1973) Optical recording of impulses in individual neurones of an invertebrate central nervous system. *Nature* **246**, 508–9.
- SALZBERG, B.M., GRINVALD, A., COHEN, L.B., DAVILA, H.V. & ROSS, W.N. (1977) Optical recording of neuronal activity in an invertebrate central nervous system: simultaneous monitoring of several neurons. *J. Neurophysiol.* **40**, 1281–91.
- SHARNOFF, M., HENRY, R.W. & BELLEZA, D.M.J. (1978a) Holographic visualization of the nerve impulse. *Biophys. J.* **21**, 109A.
- SHARNOFF, M., ROMER, N.J., COHEN, L.B., SALZBERG, B.M., BOYLE, M.B. & LESHER, S. (1978b) Differential holography of squid giant axons during excitation and rest (abstract). *Biol. Bull.* **155**, 465–6.
- SHAW, R. (1979) Photographic detectors. *Appl. Optics Optical Eng.* **7**, 121–54.
- SHEREBRIN, M.H. (1972) Changes in infrared spectrum of nerve during excitation. *Nature* **235**, 122–4.
- SHEREBRIN, M.H., MACCLEMMENT, B.A.E. & FRANKO, A.J. (1972) Electric-field induced shifts in the infrared spectrum of conducting nerve axons. *Biophys. J.* **12**, 977–89.
- SHRAGER, P., CHIU, S.Y., RITCHIE, J.M., ZECEVIC, D. & COHEN, L.B. (1987) Optical measurement of propagation in normal and demyelinated frog nerve. *Biophys. J.* **51**, 351–5.
- SIEGEL, M.S. & ISACOFF, E.Y. (1997) A genetically encoded optical probe of membrane voltage. *Neuron* **19**, 735–41.
- TANK, D. & AHMED, Z. (1985) Multiple-site monitoring of activity in cultured neurons. *Biophys. J.* **47**, 476A.
- TSAU, Y., WU, J.Y., HOPP, H.P., COHEN, L.B., SCHIMINOVICH, D. & FALK, C.X. (1994) Distributed aspects of the response to siphon touch in *Aplysia*: spread of stimulus information and cross-correlation analysis. *J. Neurosci.* **14**, 4167–84.
- TSAU, Y., WENNER, P., O'DONOVAN, M.J., COHEN, L.B., LOEW, L.M. & WUSKELL, J.P. (1996) Dye screening and signal-to-noise ratio for retrogradely transported voltage-sensitive dyes. *J. Neurosci. Methods* **70**, 121–9.
- WAGGONER, A.S. (1979) Dye indicators of membrane potential. *Annu. Rev. Biophys. Bioeng.* **8**, 47–68.
- WAGGONER, A.S. & GRINVALD, A. (1977) Mechanisms of rapid optical changes of potential sensitive dyes. *Ann. NY. Acad. Sci.* **303**, 217–41.
- WENNER, P., TSAU, Y., COHEN, L.B., O'DONOVAN, M.J. & DAN, Y. (1996) Voltage sensitive dye recording using retrogradely transported dye in the chicken spinal cord: staining and signal characteristics. *J. Neurosci. Methods* **70**, 111–20.
- WU, J.Y. & COHEN, L.B. (1993) Fast multisite optical measurements of membrane potential. In *Fluorescent and Luminescent Probes for Biological Activity* (edited by MASON, W.T.), p. 389–404. London: Academic Press.
- WU, J.Y., COHEN, L.B. & FALK, C.X. (1994a) Neuronal activity during different behaviours suggests a distributed neuronal organization in the *Aplysia* abdominal ganglion. *Science* **263**, 820–3.
- WU, J.Y., TSAU, T., HOPP, H.P., COHEN, L.B., TANG, A.C. & FALK, C.X. (1994b) Consistency in nervous systems: trial-to-trial and animal-to-animal variations in the response to repeated application of a sensory stimulus in *Aplysia*. *J. Neurosci.* **14**, 1366–84.
- YUSTE, R. & DENK, W. (1995) Dendritic spines as basic functional units of neuronal integration. *Nature* **375**, 682–4.
- ZECEVIC, D., WU, J.Y., COHEN, L.B., LONDON, J.A., HOPP, H.P. & FALK, C.X. (1989) Hundreds of neurons in the *Aplysia* abdominal ganglion are active during the gill-withdrawal reflex. *J. Neurosci.* **9**, 3681–9.